

Phase-field simulation of the effect of yield stress on the martensitic transformation in low-carbon steels

Yuhki Tsukada^{1,2*}, Emi Harata¹, Toshiyuki Koyama¹

¹ Department of Materials Design Innovation Engineering, Graduate School of Engineering,
 Nagoya University, Furo-cho, Chikusa-ku, Nagoya 464-8603, Japan

² JST, PRESTO, 4-1-8 Honcho, Kawaguchi, Saitama 332-0012, Japan

Abstract: We construct a phase-field model that considers the elastic energy derived from the fcc→bct crystal lattice deformation and slip deformation during the martensitic transformation (MT) in low-carbon steels. The MTs at 650 K and 700 K in Fe-0.1mass%C steel are simulated to examine the effect of the yield stress magnitude on the martensite microstructure. It is found that the variant domain size of the martensite phase decreases with increasing the yield stress magnitude at 650 K, but it is independent of the yield stress condition at 700 K.

1. INTRODUCTION

During the martensitic transformation (MT) in low-carbon steels, a high dislocation density is introduced into the martensite (α') phase [1,2]. The elastic energy during the MT influences the size and morphology of the α' phase. A phase-field simulation study [3] revealed that the slip deformation of the α' phase during the MT had an important role in the $(111)_\gamma$ habit plane formation. On the other hand, it has been reported that the slip deformation occurs in the surrounding austenite (γ) phase during the MT [4]. The precise knowledge on the effect of the slip deformation of the α' and γ phases on the MT is essential for the microstructure control. In this study, we construct a phase-field model that considers the elastic energy derived from the fcc→bct crystal lattice deformation and the slip deformation of the α' and γ phases during the MT. In a microstructure simulation, a yield stress value is assumed and the slip deformation is calculated in the region where the von Mises yield criterion is exceeded. The yield stress value is changed and its effect on the MT is examined by phase-field simulations.

2. CALCULATION METHOD

2.1. Phase-field model

Long-range order parameters $\{\phi_i(\mathbf{r}, t)\} = \phi_1(\mathbf{r}, t), \phi_2(\mathbf{r}, t), \phi_3(\mathbf{r}, t)$ ($i = 1, 2, 3$ numbering tetragonal variant domains of the α' phase), density functions for dislocation $\{^{(i)}p_{\alpha'}^{(m)}(\mathbf{r}, t)\} = ^{(i)}p_{\alpha'}^{(1)}(\mathbf{r}, t), ^{(i)}p_{\alpha'}^{(2)}(\mathbf{r}, t), \dots$ ($m = 1, 2, \dots$ numbering slip systems in the α' phase) and $\{p_\gamma^{(n)}(\mathbf{r}, t)\} = p_\gamma^{(1)}(\mathbf{r}, t), p_\gamma^{(2)}(\mathbf{r}, t), \dots$ ($n = 1, 2, \dots$ numbering slip systems in the γ phase) are adopted as field variables. $\phi_i(\mathbf{r}, t)$ represents the structural density of each of the three tetragonal variant domains derived from the fcc→bct crystal lattice deformation. $\phi_i(\mathbf{r}, t)$ is equal to unity if the vector \mathbf{r} is inside a variant domain of i and is zero otherwise. $^{(i)}p_{\alpha'}^{(m)}(\mathbf{r}, t)$ and $p_\gamma^{(n)}(\mathbf{r}, t)$ are in inverse proportion to the average spacing between neighboring sheared regions by dislocations $^{(i)}D_{\alpha'}^{(m)}(\mathbf{r}, t)$ and $D_\gamma^{(n)}(\mathbf{r}, t)$, respectively:

$$^{(i)}p_{\alpha'}^{(m)}(\mathbf{r}, t) = \left| \mathbf{b}_{\alpha'}^{(m)} \right| / ^{(i)}D_{\alpha'}^{(m)}(\mathbf{r}, t), \quad (1)$$

$$p_\gamma^{(n)}(\mathbf{r}, t) = \left| \mathbf{b}_\gamma^{(n)} \right| / D_\gamma^{(n)}(\mathbf{r}, t), \quad (2)$$

where and $^{(i)}\mathbf{b}_{\alpha'}^{(m)}$ and $\mathbf{b}_\gamma^{(n)}$ are the Burgers vectors. The temporal evolution of field variables is given by the following equations [5]:

$$\frac{\partial \phi_i(\mathbf{r}, t)}{\partial t} = -L_\phi \frac{\delta G}{\delta \phi_i(\mathbf{r}, t)}, \quad (3)$$

* Corresponding author. E-mail: tsukada.yuhki@material.nagoya-u.ac.jp, telephone: +81 52 789 3228.

$$\frac{\partial^{(i)} p_{\alpha'}^{(m)}(\mathbf{r}, t)}{\partial t} = -L_p \frac{\delta G}{\delta^{(i)} p_{\alpha'}^{(m)}(\mathbf{r}, t)}, \quad (4)$$

$$\frac{\partial p_{\gamma}^{(n)}(\mathbf{r}, t)}{\partial t} = -L_p \frac{\delta G}{\delta p_{\gamma}^{(n)}(\mathbf{r}, t)}, \quad (5)$$

where L_{ϕ} and L_p are kinetic coefficients, and G is the total free energy of microstructure. The G is formulated as a functional of field variables:

$$G = \int_{\mathbf{r}} \left[\frac{A}{2} \sum_{i=1}^3 \phi_i^2 - \frac{B}{3} \sum_{i=1}^3 \phi_i^3 + \frac{C}{4} \left(\sum_{i=1}^3 \phi_i^2 \right)^2 + \frac{\kappa_{\phi}}{2} \sum_{i=1}^3 (\nabla \phi_i)^2 \right. \\ \left. + \frac{\kappa_p}{2} \sum_{i=1}^3 \sum_m \left\{ {}^{(i)} \mathbf{n}_{\alpha'}^{(m)} \times \nabla^{(i)} p_{\alpha'}^{(m)} \right\}^2 + \frac{\kappa_p}{2} \sum_n \left\{ \mathbf{n}_{\gamma}^{(n)} \times \nabla p_{\gamma}^{(n)} \right\}^2 \right] d\mathbf{r} + E_{\text{el}}, \quad (6)$$

where A, B, C are Landau energy coefficients, κ_{ϕ} and κ_p are gradient energy coefficients, ${}^{(i)} \mathbf{n}_{\alpha'}^{(m)}$ and $\mathbf{n}_{\gamma}^{(n)}$ are unit vectors of the slip plane normal, and E_{el} is the elastic energy. The E_{el} is given by

$$E_{\text{el}} = \int_{\mathbf{r}} \left[\frac{1}{2} C_{klpq} \left\{ \varepsilon_{kl}(\mathbf{r}, t) - \varepsilon_{kl}^0(\mathbf{r}, t) \right\} \left\{ \varepsilon_{pq}(\mathbf{r}, t) - \varepsilon_{pq}^0(\mathbf{r}, t) \right\} \right] d\mathbf{r}, \quad (7)$$

$$\varepsilon_{kl}^0 = \sum_{i=1}^3 \left\{ \varepsilon_{kl}^{(i)} \phi_i + \sum_m \frac{{}^{(i)} \mathbf{n}_{\alpha'}^{(m)} \otimes {}^{(i)} \mathbf{b}_{\alpha'}^{(m)} + {}^{(i)} \mathbf{b}_{\alpha'}^{(m)} \otimes {}^{(i)} \mathbf{n}_{\alpha'}^{(m)}}{2 |{}^{(i)} \mathbf{b}_{\alpha'}^{(m)}|} {}^{(i)} p_{\alpha'}^{(m)} \right\} + \sum_n \frac{\mathbf{n}_{\gamma}^{(n)} \otimes \mathbf{b}_{\gamma}^{(n)} + \mathbf{b}_{\gamma}^{(n)} \otimes \mathbf{n}_{\gamma}^{(n)}}{2 |\mathbf{b}_{\gamma}^{(n)}|} p_{\gamma}^{(n)}. \quad (8)$$

In Eq. 7, C_{klpq} is the elastic constant, ε_{kl} is the total strain, and ε_{kl}^0 is the eigenstrain [6]. The eigenstrain given by Eq. 8 considers the fcc→bcc crystal lattice deformation and the slip deformation of the α' and γ phases. The transformation strain $\varepsilon_{kl}^{(i)}$ is calculated from the lattice parameters of the α' and γ phases [3].

2.2. Simulation conditions

The MTs in Fe-0.1mass% C alloy were simulated at 650 K and 700 K. $64 \times 64 \times 64$ computational grids were used for three-dimensional simulations. Unit grid size was set as $l_0 \sim 5.76$ nm (the system size was $369 \times 369 \times 369$ nm³). The periodic boundary condition was assumed along all three dimensions. We assumed the heterogeneous nucleation of the α' phase at a dislocation loop in an undercooled γ phase [7] and simulation was started by placing an α' variant domain at the center of the computational cell. Landau energy coefficients were set as $A = 32\Delta G^*$, $B = 96\Delta G^* + 12\Delta G$ and $C = 64\Delta G^* + 12\Delta G$ [8], where ΔG is the driving force for the MT. ΔG^* is the Gibbs energy barrier, which is related to the interface energy γ and gradient energy coefficient κ_{ϕ} through $\Delta G^* = 9\gamma^2 V_m / 16\kappa_{\phi}$, where V_m is the molar volume. The Gibbs energy difference between the α' and γ phases was estimated from the Thermo-Calc TCFE8 database and was used as ΔG . Note that the Gibbs energy of the ferrite phase was used as that of the α' phase. The interface energy $\gamma = 0.24$ J m⁻² was employed [9]. The gradient energy coefficients were set as $\kappa_{\phi} = 6.65 \times 10^{-14}$ J m² mol⁻¹ and $\kappa_p = 6.25 \times 10^{-13}$ J m² mol⁻¹. For simplicity, the isotropic and elastically homogeneous system was assumed. Temperature and composition dependencies of lattice parameters and elastic constants were considered [10-15]. Slip deformation of $\{101\}\langle 111 \rangle_{\alpha'}$ and $\{111\}\langle 110 \rangle_{\gamma}$ slip systems were considered. Eqs. 4 and 5 were solved in the region where the von Mises yield criterion was exceeded. The magnitude of the yield stress σ_y was changed from 0 MPa to 500 MPa and its effect on the microstructure evolution was examined. The slip deformation in the γ phase was assumed to be inherited by the α' phase during the MT.

3. RESULTS AND DISCUSSION

Fig. 1 shows the simulation results of MT at 600 K when the yield stress is assumed as $\sigma_y = 0$ MPa. Three different colors represent three tetragonal variants of the α' phase. It is seen from Fig. 1 that

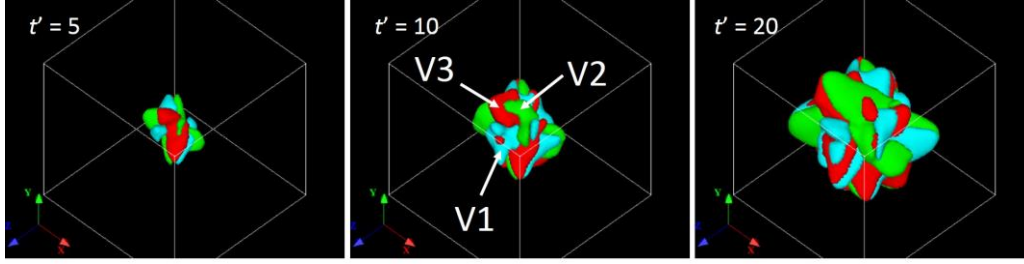


Fig. 1. Simulation results of martensitic transformation at 600 K. The yield stress is assumed as $\sigma_y = 0$ MPa. Three different colors represent three tetragonal variants of the α' phase. t' represents the dimensionless time step in the numerical analysis.

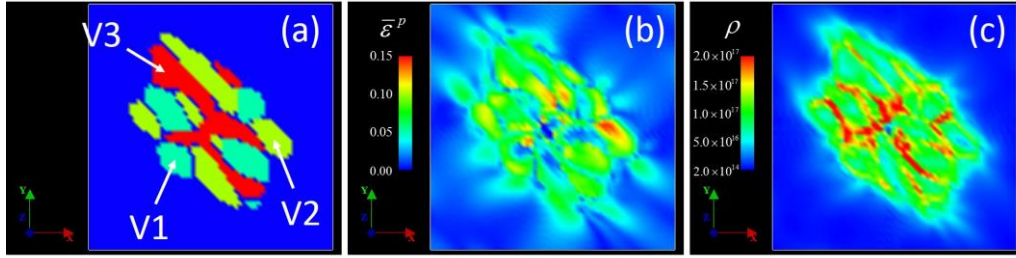


Fig. 2. $(001)_\gamma$ cross-section of the variant domain structure when the α' volume fraction is 10% (a), distribution of the equivalent plastic strain (b), and distribution of the dislocation density (c).

the MT progresses with forming the multi-variant self-accommodating structure. It has been reported that the formation of multi-variant structure is effective for relaxing a part of the elastic energy associated with the MT [16]. Fig. 2(a) shows a $(001)_\gamma$ cross-section of the variant domain structure when the α' volume fraction is 10%. The distributions of the equivalent plastic strain and dislocation density on the corresponding $(001)_\gamma$ cross-section are shown in Fig. 2(b) and 2(c), respectively. Note that dislocations are assumed to occur at places where the spatial gradient of ${}^{(i)}p_\alpha^{(m)}(\mathbf{r}, t)$ and $p_\gamma^{(n)}(\mathbf{r}, t)$ exists [3], and the dislocation density is calculated as

$$\rho(\mathbf{r}, t) = \sum_{i=1}^3 \sum_m \frac{|\mathbf{n}_\alpha^{(m)} \times \nabla {}^{(i)}p_\alpha^{(m)}(\mathbf{r}, t)|}{|\mathbf{b}_\alpha^{(m)}|} + \sum_n \frac{|\mathbf{n}_\gamma^{(n)} \times \nabla p_\gamma^{(n)}(\mathbf{r}, t)|}{|\mathbf{b}_\gamma^{(n)}|}. \quad (9)$$

We see from Fig. 2(b) that the plastic strain is large in the interior of the α' variant domains. Furthermore, it can be confirmed that the plastic strain also occurs in the γ phase near the interface between the α' and γ phases. On the other hand, in contrast to the plastic strain distribution, the dislocation density is high at interfaces between different α' variant domains (Fig. 2(c)). The slip deformation of the α' phase during the MT is presumed to cause the rotation of the crystallographic orientation of the α' phase. This might have an important role in the formation process of the Kurdjumov–Sachs orientation variants in low-carbon steels [17].

Fig. 3 shows the multi-variant domain structure and each variant domain structure of the α' phase simulated at 600 K when the yield stress is assumed as $\sigma_y = 400$ MPa. It can be seen that the α' phase grows along the

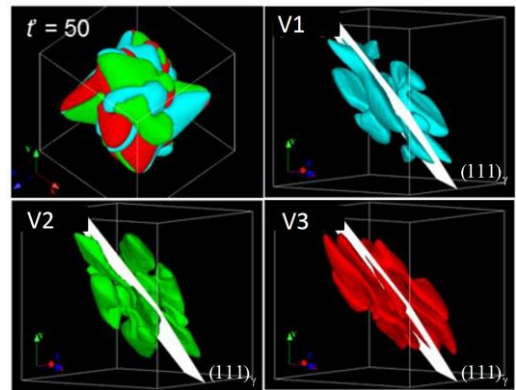


Fig. 3. Multi-variant domain structure and each variant domain structure of the α' phase simulated at 600 K. The yield stress is assumed as $\sigma_y = 400$ MPa.

(111)_γ plane and the (111)_γ habit plane is formed. Furthermore, it is interesting to note that the interface between different α' variant domains is also formed near the (111)_γ plane. This characteristic morphology of the α' variant domain structure is simulated only when the slip deformation is considered in both of the α' and γ phases. In our simulations at two temperatures (650 K and 700 K) and under various yield stress conditions (0~500 MPa), the formation of the (111)_γ habit plane is clearly observed when the simulation was performed at 600 K and the yield stress is assumed as $\sigma_y = 300\sim 500$ MPa.

We counted the total number of isolated variant domains on {100}_γ cross-sections and used it as a measure of the α' variant domain size. Fig. 4 shows the effect of the yield stress magnitude on the total number of isolated α' variant domains on 192 cross-sections. It is seen that at 650 K, the variant domain size decreases with increasing the yield stress magnitude. On the other hand, at 700 K, the variant domain size is not so influenced by the yield stress condition. When the transformation temperature is high, the driving force for the MT is small and the transformation is slowed down. This would secure sufficient time for the slip deformation during the MT and would lead to the increase in the amount of plastic strain in the α' phase. It is presumed that at 700 K, a large amount of plastic strain in the α' phase relaxes the elastic energy associated with the MT and decreases the tendency of self-accommodation.

4. CONCLUSIONS

Phase-field simulations were performed to examine the effect of the yield stress magnitude on the MTs at 650 K and 700 K in Fe-0.1mass%C steel. Obtained results are summarized as follows: (1) when the yield stress is assumed as $\sigma_y = 300\sim 500$ MPa at 600 K, interfaces between different α' variant domains are formed near the (111)_γ plane; (2) the plastic strain is large in the interior of the α' variant domains; (3) the dislocation density is high at interfaces between different α' variant domains; (4) the variant domain size of the α' phase decreases with increasing the yield stress magnitude at 650 K, but it is independent of the yield stress condition at 700 K.

Acknowledgement: This work was supported by JST PRESTO (Grant Number JPMJPR15NB).

REFERENCES

- [1] M. Kehoe and P.M. Kelly: *Scr. Metall.*, 4 (1970), 473–476.
- [2] S. Morito, J. Nishikawa and T. Maki: *ISIJ Int.*, 43 (2003), 1475–1477.
- [3] Y. Tsukada, Y. Kojima, T. Koyama and Y. Murata: *ISIJ Int.*, 55 (2015), 2455–2462.
- [4] G. Miyamoto, A. Shibata, T. Maki and T. Furuhashi: *Acta Mater.*, 57 (2009), 1120–1131.
- [5] L.Q. Chen: *Ann. Rev. Mater. Res.*, 32 (2002), 113–140.
- [6] A.G. Khachaturyan: *Theory of Structural Transformations in Solids*, Dover, New York (2008).
- [7] W. Zhang, Y.M. Jin and A.G. Khachaturyan: *Acta Mater.*, 55 (2007), 565–574.
- [8] H.K. Yeddu, A. Malik, J. Ågren, G. Amberg and A. Borgstrom: *Acta Mater.*, 60 (2012), 1538–1547.
- [9] Z. Yang and R.A. Johnson: *Model. Simul. Mater. Sci. Eng.*, 1 (1993), 707–716.
- [10] C.S. Roberts: *Trans. AIME*, 197 (1953), 203–204.
- [11] L. Cheng, A. Böttger, T.H. Keijsers and E.J. Mittemeijer: *Scr. Metall. Mater.*, 24 (1990), 509–514.
- [12] I. Seki and K. Nagata: *ISIJ Int.*, 45 (2005), 1789–1794.
- [13] *Kinzoku Data Book*, 4th rev. ed., ed. by The Japan Institute of Metals, Maruzen, Tokyo (2004).
- [14] G.R. Speich, A.J. Schwobele and W.C. Leslie: *Metall. Trans.*, 3 (1972), 2031–2037.
- [15] D.J. Dever: *J. Appl. Phys.*, 43 (1972), 3293–3301.
- [16] L. Qi, A.G. Khachaturyan and J.W. Morris Jr.: *Acta Mater.*, 76 (2014), 23–39.
- [17] S. Morito, H. Tanaka, R. Konishi, T. Furuhashi and T. Maki: *Acta Mater.*, 51 (2003), 1789–1799.

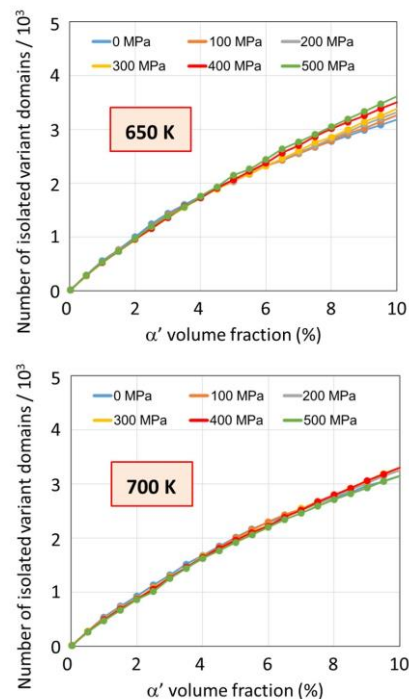


Fig. 4. Effect of yield stress magnitude on the total number of isolated α' variant domains on {100}_γ cross-sections.